*Journal of The Electrochemical Society*, **149** (9) A1121-A1126 (2002)
0013-4651/2002/149(9)/A1121/6/$7.00 © The Electrochemical Society, Inc.



# Interfacial Stability Between Lithium and Fumed Silica-Based Composite Electrolytes

**Jian Zhou,* Peter S. Fedkiw,**,z and Saad A. Khan**

*Department of Chemical Engineering, North Carolina State University, Raleigh, North Carolina 27695-7905, USA*

Composite electrolytes consisting of methyl-capped poly(ethylene glycol) oligomer (Mw ≈ 250), lithium bis(trifluoromethylsulfonyl)imide (Li:O = 1:20), and fumed silica were investigated. In particular, the effects of fumed silica-surface chemistry and weight percentage in the composite on cycling behavior of Li/electrolyte/Li, Li(Ni)/electrolyte/Li, and Li/electrolyte/metal oxide cells were studied. Four types of fumed silicas with various surface groups were employed, A200 (native hydroxyl groups), R805 (octyl-modified), R974 (methyl-modified), and FS-EG3 (ethylene oxide-modified). The presence of fumed silica enhances lithium cyclability by reducing the interfacial resistance and cell-capacity fading, regardless of surface chemistry. However, the extent of the enhancing effect of fumed silica strongly depends on its surface chemistry, with the largest effect seen with A200 and the least effect seen with FS-EG3. Increasing fumed silica weight fraction intensifies the stabilizing effect.
 [DOI: 10.1149/1.1496483] 

Manuscript submitted December 10, 2001; revised manuscript received Febraury 25, 2002. Available electronically July 16, 2002.

Although lithium metal is an attractive anode material for rechargeable batteries because of its high specific energy, the commercialization of rechargeable lithium batteries is impeded by its high reactivity with electrolyte components. One way to overcome this limitation without sacrificing energy density is to develop suitable electrolytes that are kinetically stable to lithium. In addition to good interfacial stability, high conductivity ($>10^{-3}$ S/cm at room temperature) and mechanical strength are also required. Among currently examined electrolytes, composite electrolytes show promising electrochemical (*e.g.*, conductivity, interfacial stability, and ionic transport properties) and mechanical properties (*e.g.*, viscous and elastic moduli, yield stress) for lithium battery applications.[1-6]

Most composite electrolytes reported in the literature are formed by dispersing ceramic fillers (*e.g.*, $Al_2O_3$, $SiO_2$, $TiO_2$) into high-molecular weight (Mw) poly(ethylene oxide) (PEO) polymers doped with lithium salts LiX.[1-4,7-16] Addition of ion-conducting (*e.g.*, γ-$LiAlO_2$,[1,3,4] $Li_3N$[4,9]) and even inert ceramic fillers (*e.g.*, $SiO_2$,[5] $TiO_2$,[16] MgO[17]) enhances the conductivity of a high Mw PEO electrolyte, with the latter attributed to an increase in volume fraction of the conductive amorphous phase due to the presence of a homogeneous dispersion of fine particles. Experimental evidence from various groups consistently shows that the interface between lithium and a composite electrolyte is more stable and efficient in cycling than the filler-free electrolyte.[1,3,4,7] The enhanced interfacial stability is suggested to be affected by the filler particles scavenging impurities such as water and oxygen,[2] which can react with lithium and thus accelerate its corrosion. However, the ionic conductivity of this type of composite electrolyte at ambient temperature is $10^{-4}$ to $10^{-5}$ S/cm, which is below the acceptable range for some applications.[3,16]

In recent years, our group has developed a new type of composite electrolyte by dispersing fumed silica (FS) into low to moderate Mw PEO.[5,6,18-20] Unlike high Mw based PEO composites, the solid-like structure is formed by the filler (fumed silica) instead of PEO chains. Earlier research has demonstrated that composites consisting of fumed silica + low Mw PEO + lithium salts are promising materials for rechargeable lithium batteries in terms of their high conductivity ($>10^{-3}$ S/cm at room temperature) and mechanical strength (elastic modulus $G' > 10^5$ Pa).[5,6,19,20] A significant improvement of lithium interfacial stability with incorporation of the fumed silica is also observed at open circuit.[5]

Fumed silica is an amorphous, nonporous form of silicon dioxide ($SiO_2$) prepared by flame hydrolysis of silicon tetrachloride.[21] The predominant particle structures of fumed silica are aggregates (*ca.* 0.1 μm long), which consist of partially fused primary particles (*ca.* 12 nm diam) and cannot be disrupted by shear.[22] This aggregated structure is responsible for the unique properties of fumed silica. The surface chemistry of fumed silica also plays a significant role and determines many macroscopic properties in applications.

In the present communication, we report our investigation of the interfacial stability between lithium and fumed silica-based composites by cycling of Li/electrolyte/Li, Li(Ni)/electrolyte/Li, and Li/electrolyte/metal oxide cells. The effects of current density, surface chemistry, and weight percentage of fumed silica are demonstrated.

Four types of fumed silicas with various surface groups are used in this study: A200 (native hydroxyl groups), R805 (octyl-modified), R974 (methyl-modified), and FS-EG3 (ethylene oxide-modified), with the first three being commercial products from Degussa (Akron, OH) and designated with the manufacturer's nomenclature and the latter synthesized at Michigan State University (MSU). Details of surface chemistries of these fumed silicas are provided in Table I, with silanol density values determined by titration with lithium aluminum hydride ($LiAlH_4$).[21,23] The surface of unmodified fumed silica (A200) contains silanols (Si-OH) to the extent of about 2.5 [SiOH] groups/nm$^2$, or equivalently about 0.84 mmol/g.[21,22] These silanols render the native fumed silica surface hydrophilic. The silanols can be replaced by reactions with various chlorosilanes, alkoxysilanes, or silazanes[24] to generate hydrophobic fumed silicas. Each of the remaining fumed silicas was synthesized using A200 as the starting material. The octyl-modified R805 is obtained by reacting A200 with octyltrimethoxysilane (OTMS), while R974 is generated by reacting A200 with dimethyldichlorosilane (DMDCS). The ethylene oxide-modified FS-EG3 is prepared by reacting A200 with chlorodimethyl(4,7,10,13-tetraoxatetradecyl)silane. The synthetic procedure for preparing FS-EG3 is given by Hou.[23] One significant difference between commercial (A200, R805, and R974) and in-house synthesized fumed silica (FS-EG3) is that the latter has considerably larger agglomerates, as determined by visual observation.

## Experimental

*Preparation of composites.*—The composite electrolytes consist of three materials, lithium bis(trifluoromethylsulfonyl)imide [$LiN(CF_3SO_2)_2$] (LiTFSI, 3M), fumed silica (Degussa, or surface-modified form synthesized at MSU[6,23]), and poly(ethylene glycol)dimetheyl ether (PEG-dm, Mw 250, Aldrich). LiTFSI was dried at 110°C under vacuum for 24 h before use. PEG-dm was dried over 4 Å molecular sieves for at least one week. The water content of both materials was controlled under 20 ppm, as determined by Karl-Fisher titration. Fumed silicas were dried at 120°C under vacuum for 3-4 days to achieve a water content of 150-200 ppm before being transferred to an argon-filled glove box.

* Electrochemical Society Student Member.
** Electrochemical Society Active Member.
z E-mail: Fedkiw@eos.ncsu.edu

**Table I. Characteristics of fumed silicas used in this study.**

| Fumed silica | Dominant surface group(s) | Fraction of surface substituted (mol %)[23,31] | Fraction of unreacted Si-OH (mol %) |
|---|---|---|---|
| A200 | Si-OH [silanol] | 0 | 100 |
| R974 | Si-$(CH_3)_2$ [di-methyl) | 50 | 50 |
| R805 | Si-$C_8H_{17}$ [octyl] | 48 | 52 |
| FS-EG3 | Si-$(CH_2)_3(O\text{-}CH_2\text{-}CH_2)_3\text{-}OCH_3$ | 35 | 65 |

Composite electrolytes were prepared in an argon-filled glove box. First, a baseline electrolyte was made by dissolving LiTFSI in PEG-dm oligomer in a fixed ratio of Li:O (1:20) (1 M LiTFSI solution) to maintain the highest conductivity.[6] A certain weight of fumed silica was then added to the baseline electrolyte and dispersed into the electrolyte by use of a high-shear mixer (Tissue Tearor™, model 398, BioSpec Products, Inc.) to get the desired concentration.[19] Water content of the baseline electrolyte and the composites was under 20 and 50 ppm, respectively. The baseline electrolyte is a liquid while composite electrolytes are solid-like gels with viscosities and transport properties reported elsewhere.[25]

*Preparation of cathodes.*—All components of the metal-oxide cathodes, $LiCoO_2$ (OM Group, Inc., OMG), $LiMn_2O_4$ (Merck), or $V_6O_{13}$ (Kerr-McGee), poly(vinylidene fluoride) (PVDF, Kynar® Flex 2800-00, Elf Atochem North America), graphite Timrex SFG15 (Timcal), and 1-methyl-2-pyrrolidinone (NMP, Aldrich) were used as received. The typical composition for a 4 V cathode ($LiCoO_2$ or $LiMn_2O_4$) is approximately 91 wt % metal oxide, 6 wt % graphite, and 3 wt % PVDF binder.[26] A 3 V cathode ($V_6O_{13}$) normally consists of 75 wt % metal oxide, 20 wt % graphite, and 5 wt % PVDF binder. Aluminum foil (0.024 mm thick, Fisher Scientific) and 0.127 mm thick sheet of carbon fiber (Techimat® 6100-035, Lydall Technical Papers) were used as the current collector for 4 V cathodes and a 3 V cathode, respectively. Usually the mixture of metal oxide and SFG15 graphite was dispersed into a solution of PVDF using NMP as solvent. The resulting slurry was coated onto the current collector by a doctor blade, and the final thickness of wet cathode films was approximately 0.20 mm for $LiCoO_2$ or $LiMn_2O_4$ and 0.30 mm for $V_6O_{13}$. The film was dried at 80°C overnight and was cut into 12.7 mm diameter disks which were hot-compacted by a hydraulic press at 150°C and 770 MPa. After compaction, cathode disks were dried at 150°C under vacuum for 24 h.

*Preparation of coin cells.*—Coin cells in which an electrolyte/separator is sandwiched between a thin sheet of lithium metal and another electrode (lithium foil, nickel foil, or metal-oxide composite cathode) are used in our cycling measurements (Fig. 1). In these cells, the Celgard® 2400 separator (25 μm thick) is either wetted by the baseline electrolyte or sandwiched between two layers of composite electrolyte. A stainless steel spacer and spring are used to maintain good contact of electrolyte, electrode, and current collector.

*Methods and measurements.*—An Arbin battery cycler (model BT2042) controlled by Arbin ABTS software is employed to carry out constant-current cell cycling. In Li/electrolyte/Li cells, current densities of 0.2 and 1.0 mA/cm$^2$ with fixed charge density of 120 mC/cm$^2$ were applied. Cell cycling was terminated upon reaching the fixed maximum cycle number of 584 or by reaching the voltage safety limit of ±10 V. In full cell cycling, cells were cycled at a constant current density of 0.08 mA/cm$^2$ between 2.5 and 4.2 V for $LiCoO_2$ cathode, 3.0 and 4.2 V for $LiMn_2O_4$ cathode, and 1.8 and 3.0 V for $V_6O_{13}$ cathode. The current density corresponds approximately to a C/40 rate for $LiCoO_2$ and $LiMn_2O_4$ cells and C/75 rate for $V_6O_{13}$ cells. In cycling the Li(Ni)/electrolyte/Li cells, a known charge was first passed through the cell at 0.2 mA/cm$^2$ to prepare the lithium electrode ($Q_D$ = 2.4 C/cm$^2$, nominal Li thickness of 3.0 μm). Then, a fraction of this charge [cycling charge, $Q_c$ = 0.24 C/cm$^2$, depth of discharge (DOD) = 10%)] was alternately cycled across the cell for 20 lithium deposition-dissolution cycles, and the lithium stripping overvoltage was monitored upon cycling. Finally, the remaining Li on the Ni surface was anodically removed during the last dissolution half-cycle, and the amount of charge passed, $Q_f$, was monitored. The cutoff voltage for the dissolution half-cycle was set at 1.5 V *vs.* Li metal. The mean value of the lithium electrode cycling efficiency, η, was calculated by[27]

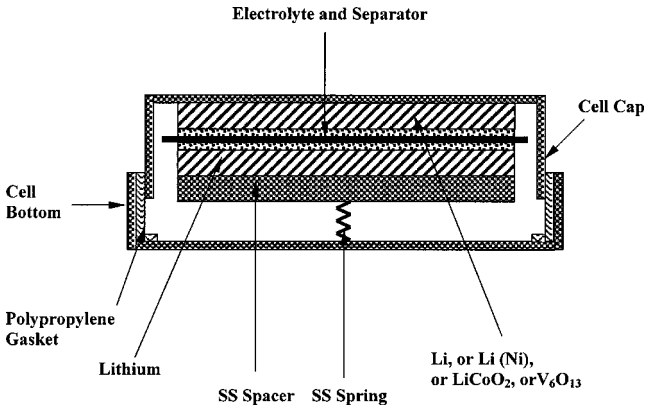


**Figure 1.** Coin cell for cycling studies (not to scale).

$$\eta = \frac{Q_c - (\eta Q_D - Q_f)/n}{Q_c} \times 100\% \qquad [1]$$

where $n$ = 20 or $n$ = actual number of cycles in which 0.24 C/cm$^2$ Li is stripped from Ni.

The lithium surface before and after Li/electrolyte/Li cycling was also studied via electrochemical impedance spectroscopy (EIS) using a Zahner impedance analyzer IM6e. Open-circuit impedance data were collected in a range of 100 kHz to 100 mHz with an ac amplitude of 10 mV. The interfacial resistance ($R_{int}$) between the lithium metal and the electrolyte was determined according to the method of Fauteux.[28]

## Results and Discussion

*Li/electrolyte/Li cycling.*—Figure 2 shows voltage waveforms in the absence of fumed silica (top) and with a composite electrolyte containing 10% R805 (bottom). The voltage of the cell with the composite electrolyte is relatively stable from cycle-to-cycle and over each half-cycle. However, the voltage of the cell without fumed silica increases dramatically after 150 cycles and also changes considerably during the half-cycle. The cells with composite electrolytes consisting of other fumed silicas (R974, A200, and FS-EG3) show similar qualitative behavior. Figure 3 compares the cycle-number dependence of the average voltage over a half-cycle of the baseline electrolyte to that of composite electrolytes with various surface groups on the fumed silica: hydroxyl (A200), methyl (R974), octyl (R805), and ethylene oxide (EO) (FS-EG3). The average voltage without fumed silica increases dramatically around 100 cycles while the average voltage of cells with composite electrolytes stays fairly constant for at least 300 cycles. The average voltage of the cell with the baseline electrolyte varies approximately 2 to 50 times that of cells with the composites and differs with fumed-silica type.

As reported earlier,[6] the conductivity of these composite electrolytes is essentially independent of surface chemistry at a given weight fraction of fumed silica; hence, the differing effect of the fumed-silica type on the average voltage of Li/electrolyte/Li cells is not due to the bulk conductivity of electrolytes, but may be attributed to the differing effect on the electrolyte/lithium interface. The

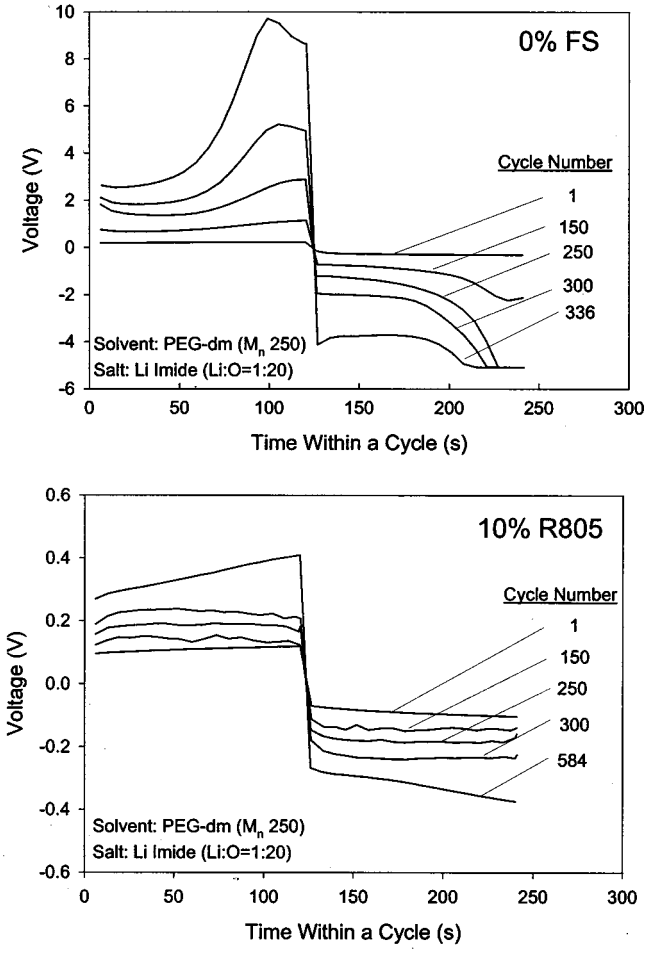


**Figure 2.** Voltage waveform of Li/electrolyte/Li cells without (top) and with (bottom) fumed silica cycled at 1 mA/cm$^2$. (FS: fumed silica; R805: octyl-modified fumed silica.)

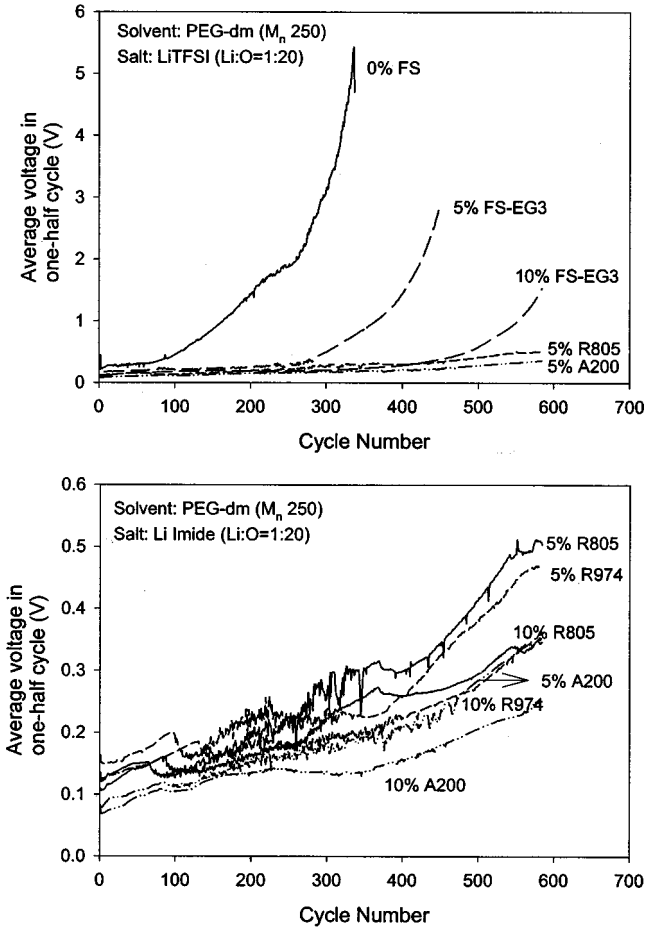


**Figure 3.** Effect of fumed silica surface chemistry on voltage response of Li/electrolyte/Li cells at 1 mA/cm$^2$. (FS: fumed silica; A200: native -OH surface groups; R805: octyl-modified fumed silica; R974: methyl-modified fumed silica; FS-EG3: ethylene oxide-modified fumed silica.)

addition of fumed silica clearly stabilizes the electrolyte and lithium metal interface, and this effect is enhanced with increased weight fraction of fumed silica. The surface chemistry of fumed silica influences the extent of improvement. With the same weight fraction, the order of improvement effect is A200 (hydroxyl group) > R974 (methyl group) > R805 (octyl group) > FS- EG3 (EO group).

The improvement effect of fumed silica was also seen in impedance measurements. The impedance of the cells was measured before and after cell cycling. Figure 4 shows typical Nyquist plots of cells with baseline electrolyte (top) and composite electrolyte (bottom). The interfacial resistance increases for both types of cells with cycle number. The interfacial resistance of the baseline electrolyte becomes almost ten times its original value after 336 cycles; the cycling had to be stopped at this point due to the safety limit of the equipment. However, the interfacial resistance of the composite electrolyte with 10% R805 is only one-fourth that of the baseline electrolyte even after 584 cycles.

Figure 5 summarizes the interfacial resistances of Li/electrolyte/Li cells without fumed silica and with various types (R805, R974, A200, and FS-EG3) before and after cycling. The interfacial resistances of the cells show the same trend as that of the average voltage. Some Li/electrolyte/Li cycling was also carried out at a higher charge density of 1 C/cm$^2$ (not shown). These data also demonstrated that fumed silica improved the electrolyte/Li interface and A200 showed a better effect than R805.

The A200 hydrophilic fumed silica of all those studied produces the most improved Li-electrolyte interface, which suggests that the hydroxyl group on the fumed silica surface does not react appreciа-

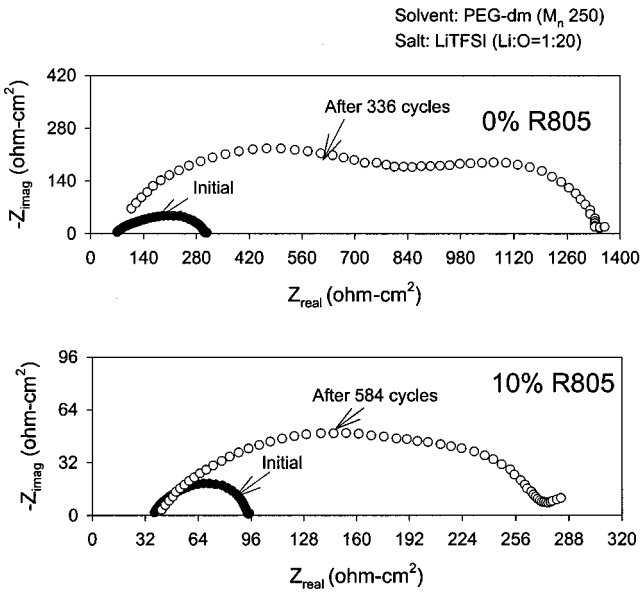


**Figure 4.** Nyquist plot of baseline (top) and composite electrolyte (bottom) systems before and after cycling Li/electrolyte/Li cells at 1 mA/cm$^2$.

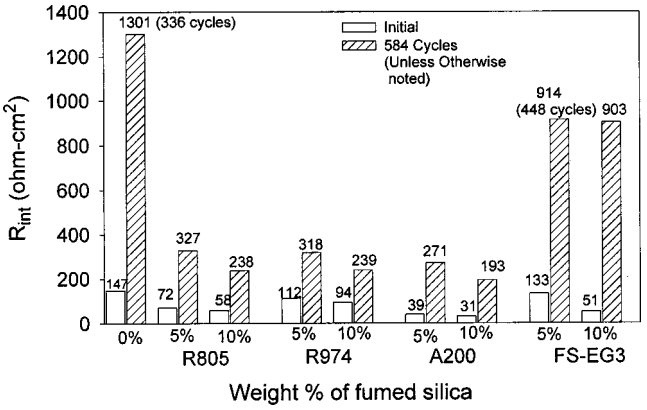


**Figure 5.** Effect of fumed silica and its surface chemistry on interfacial resistance for cycled cells shown in Fig. 3.

bly with lithium. Otherwise, we would anticipate that A200 has the least beneficial effect since it has the highest content of surface hydroxyl groups (100%). It has been suggested that the improvement of the electrolyte and lithium metal interface affected by ceramic fillers is due to the fillers' scavenging of impurities in electrolyte materials such as $H_2O$ and $O_2$ and shielding lithium from corrosion by forming compact thin passivation layers on its surface.[2,29,30] The A200 hydrophilic fumed silica has greater adsorption of $H_2O$ than hydrophobic fumed silicas such as R805 and R974; therefore, based on these effects A200 is expected to have a better improvement effect than R805 and R974.

Although R805 and R974 have nearly the same coverage of surface hydroxyl (48 and 50%, respectively), the hydroxyl on R974 is less shielded by the shorter methyl groups than longer octyl chains on R805.[31] Therefore, R974 has a better improvement effect than R805 because of a greater accessibility of surface OH groups, which is supported by a lower degree of hydrophobicity of R974 than R805.[32]

EO-modified fumed silica FS-EG3 also stabilizes the electrolyte and lithium metal interface, indicating that the ethylene oxide chain attached to the fumed silica apparently does not react appreciably with lithium metal. However, we see less improvement with FS-EG3 than the other fumed silicas, which might be explained by several reasons. Although FS-EG3 has the highest molar fraction of silanol groups at the surface among the hydrophobic fumed silicas tested, accessible silanol groups per unit weight are believed to be less than those of R974 and R805. Earlier research of fumed silica fillers in different organic solvents showed that the interaction between surface chains is the cause of gel formation in these systems, and the surface interaction deteriorates when their solvency in the continuous medium is enhanced.[31,33] PEG-dm (250) acts as a good solvent for FS-EG3 due to the compatibility between surface groups of FS-EG3 and PEG-dm (250) solvent. We postulate that the solvent-fumed-silica-surface interaction prevails over fumed-silica/fumed-silica-surface interaction in the FS-EG3 system. Because of the strong solvent-surface interaction, PEG-dm molecules form a solvation layer on each silica unit and shield surface silanol groups from mutual interaction or interaction with other molecules. In addition, FS-EG3 has a larger agglomerate size than other fumed silicas. It is recognized[4,14,29,34,35] that particle size of ceramic fillers plays a significant role in electrochemical properties of composite electrolytes such as conductivity, interfacial stability, and ionic transport, which are improved when particle size drops. Hence, the larger agglomerate size further lowers the improvement effect of FS-EG3 on electrolyte/lithium interfacial stability. The precise mechanism that dictates different effects of various fumed silica on interfacial stability is unresolved and is a focus of ongoing efforts.

The above discussion compared the cell-cycling behavior at 1.0 mA/cm$^2$, which is a fairly high rate for rechargeable lithium batteries. As a means to determine to what extent current density influences the improvement effect of fumed silica, we cycled cells at 0.2 mA/cm$^2$ with 0, 5, and 10% R805 present in the electrolytes. The results showed that current density greatly influences the effect of fumed silica on interfacial stability. Figure 6 shows average voltage *vs.* cycle number at 0.2 mA/cm$^2$ (top) and at 1.0 mA/cm$^2$ (bottom). Again, cells with a composite electrolyte show a more stable interface at 0.2 mA/cm$^2$. Also a higher weight fraction of fumed silica gives lower average voltage and interfacial resistance. However, we see less improvement of the interface at a lower current density; that is, the difference in cells with and without fumed silica is not as pronounced as at 1.0 mA/cm$^2$. According to the study of Arakawa *et al.* on the effect of charging current density on lithium morphology,[36] a lithium surface is smoother at a lower rate, and the available lithium surface for the solvent, lithium salt, and impurities to react within a unit time is less. Thus, the corrosion of the lithium metal is not as severe as that at higher current density. Therefore, even the baseline electrolyte shows a more stable interface at a lower current density. However, we still observe an improvement of the interface by the addition of the fumed silica.

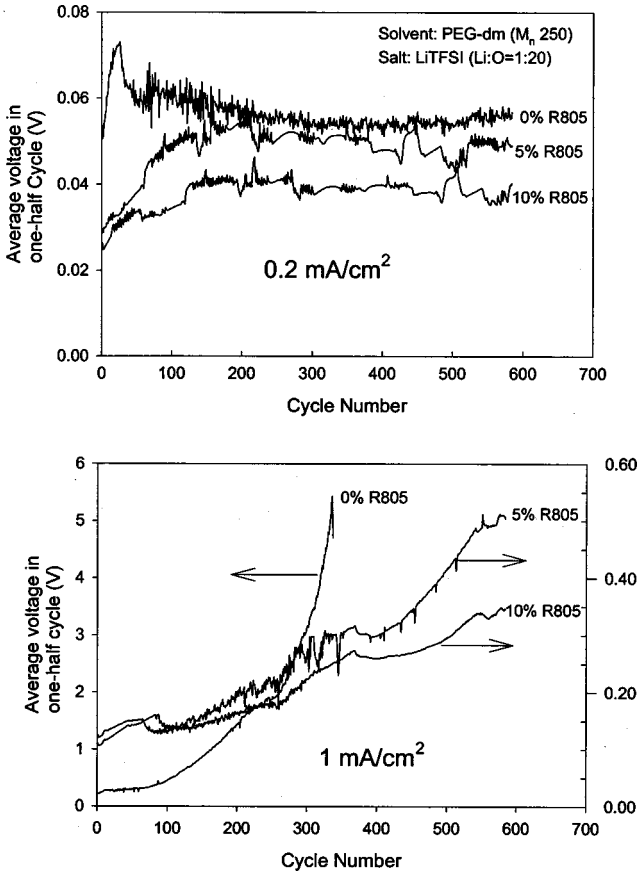


**Figure 6.** Effect of current density on cycling behavior of Li/electrolyte/Li cells for baseline and composite systems.

*Li(Ni)/electrolyte/Li cycling.*—In the above Li/electrolyte/Li cycling, the total amount of available lithium is several hundred to thousand times of the amount of lithium actually cycled (560 C/cm$^2$ *vs.* 120 mC/cm$^2$ or 1 C/cm$^2$). It is not possible to determine lithium cycling efficiency and cycleability from such studies. Accordingly, a Li(Ni)/electrolyte/Li cell with a controlled amount of excess lithium was employed (nine times excess of lithium cycled). Figure 7 shows Li(Ni)/electrolyte/Li cycling results at 0.2 mA/cm$^2$ and illustrates that deposited Li becomes ''dead Li'' after the first three cycles in the absence of fumed silica, but the addition of 10 wt % of R805

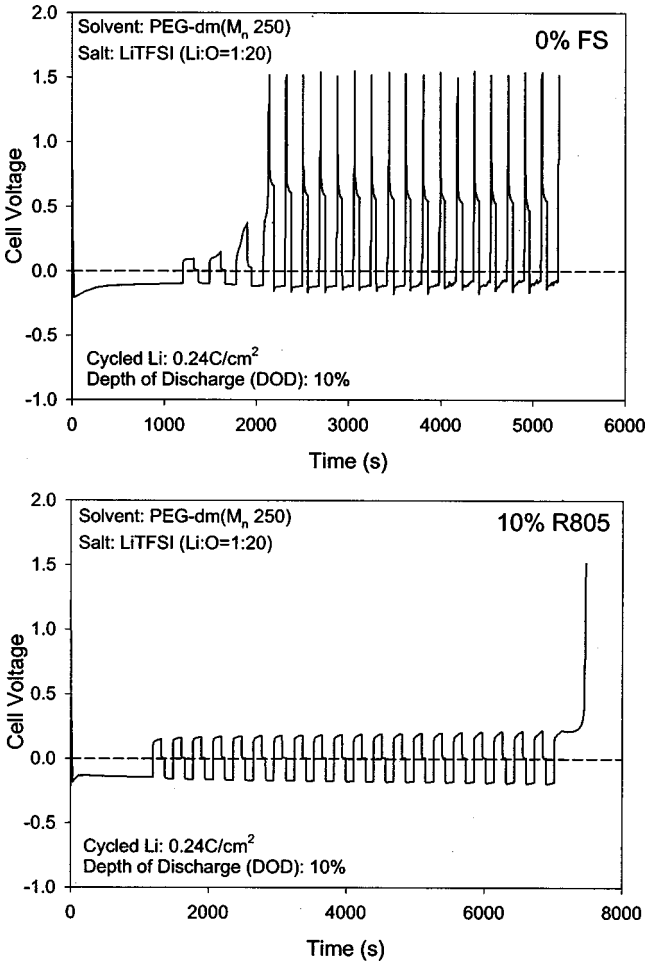


**Figure 7.** Effect of fumed silica on cycling behavior of Li(Ni)/electrolyte/Li cells without (top) and with (bottom) fumed silica.

improves Li cyclability dramatically. Thus, $n = 3$ is used in the cycling efficiency calculation for baseline electrolyte instead of 20 in the case of 10% R805 composite electrolyte. The cycling efficiency of baseline electrolyte for three cycles is 25% due to the fast loss of cyclable Li. However, the cycling efficiency of 10% R805 composite is about 70% for 20 cycles under the same experimental conditions. This significant improvement of cycling efficiency of composite electrolyte can be also attributed to the stabilizing effect of fumed silica to the electrolyte-lithium interface.

*Full-cell cycling.*—The effect of fumed silica surface chemistry on full-cell cycling behavior was studied using a standard $LiCoO_2$ cathode composition (91% $LiCoO_2$, 6% graphite SFG 15, and 3% PVDF) at a C/40 rate (Fig. 8). Three types of fumed silica were used, native hydroxyl group A200, octyl-modified R805, and EO-modified FS-EG3. Cell capacity quickly fades after the first few cycles in the absence of fumed silica but addition of 10 wt % particulates diminishes the capacity fade, with the effect dependent upon the silica-surface chemistry. The native fumed silica, A200, shows the best improvement while EO-modified fumed silica FS-EG3 shows the least effect. This trend agrees with the Li/electrolyte/Li cycling results.

A different cathode material does not alter the beneficial effect of fumed silica on full-cell cycling behavior. Figure 9 shows charge and discharge behavior of rechargeable lithium cells using lithium manganese oxide cathodes at a C rate of C/40 with 10% R805 composite and its baseline electrolyte. From Fig. 9, we see that the addition of fumed silica again improves discharge capacity. In addition, a cell with 10% R805 shows less capacity fading. These improvements may be due to the enhancement of the interfacial stability between composite electrolyte and lithium metal.

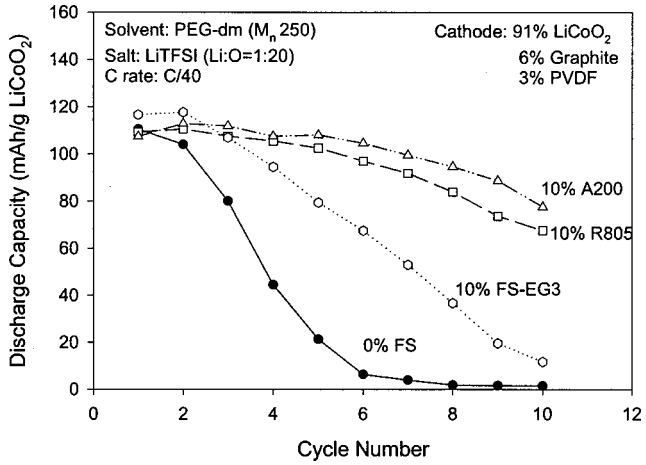


**Figure 8.** Effect of fumed silica surface chemistry on full cell cycling of Li/electrolyte/$LiCoO_2$ cells at C/40 ($i = 0.08$ mA/cm$^2$).

Although the presence of fumed silica increases discharge capacity and reduces capacity fading in 4 V lithium metal cells, the capacity fading is still severe even in the best case, *i.e.*, 27% after ten cycles for 10% A200 composite system with a $LiCoO_2$ cathode. Since our baseline and composite electrolytes are electrochemically stable up to 5.5 V,[5] severe capacity fading is possibly due to the pitting corrosion of aluminum cathode current collector induced by TFSI anion at potentials greater than 3.5 V *vs.* Li.[37-39] In order to increase the capacity stability of electrolytes containing LiTFSI salt, a 3 V cathode material $V_6O_{13}$ was employed in full-cell cycling studies. Figure 10 shows cell cycling behavior of the cell with baseline electrolyte, 10% R805 and 10% A200 composite electrolytes at C/75 (0.08 mA/cm$^2$). As shown in Fig. 10, the capacity for the first discharge cycle of Li/$V_6O_{13}$ cells is as high as 297 mAh/g (5.7 Li/$V_6O_{13}$) for baseline electrolyte, 306 mAh/g (5.8 Li/$V_6O_{13}$) for 10% R805 composite electrolyte, and 321 mAh/g (6.1 Li/$V_6O_{13}$) for 10% A200 composite electrolyte. The capacity of the cell using 10% A200 composite electrolyte is the highest throughout cycling, followed by 10% R805 composite and baseline electrolyte. Capacity differences between cells increase from the initial values after eight cycles. From Fig. 8 and 9, we see that discharge capacity of 4 V

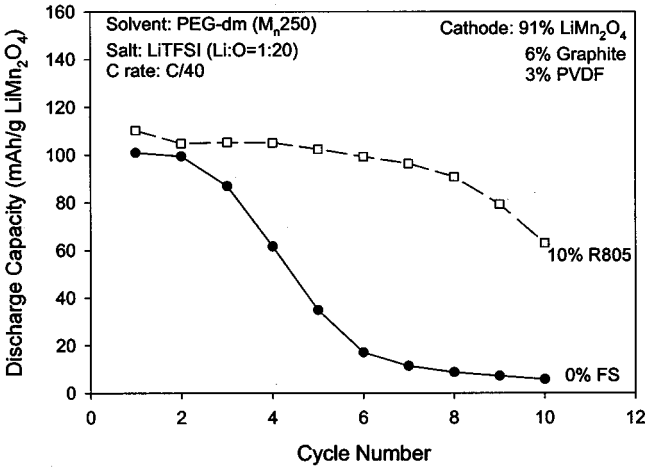


**Figure 9.** Effect of fumed silica surface chemistry on full cell cycling of Li/electrolyte/$LiMn_2O4$ cells at C/40 ($i = 0.08$ mA/cm$^2$).

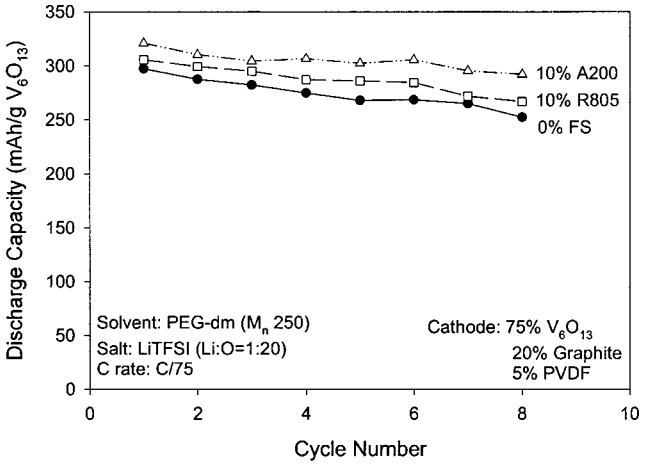


**Figure 10.** Effect of fumed silica surface chemistry on full cell cycling of Li/electrolyte/$V_6O_{13}$ cells at C/75 ($i$ = 0.08 mA/cm$^2$).

lithium cells decays dramatically after three or four cycles and decreases to essentially zero after six cycles in the absence of fumed silica. Unlike 4 V lithium cells, the discharge capacity of a Li/$V_6O_{13}$ cell with a baseline electrolyte does not drop significantly after three or four cycles. It remains fairly high even after eight cycles, 252 mAh/g (4.8 Li/$V_6O_{13}$). The switch from 4 to 3 V cathode material apparently reduces capacity fade of the baseline electrolyte system. As seen in 4 V cells, fumed silica also shows beneficial effects of increasing discharge capacity and diminishing the capacity fading seen in 3 V cells. Again, A200 shows a stronger improvement than R805.

## Conclusions

Li/electrolyte/Li, Li(Ni)/electrolyte/Li, and full cell cycling data show that fumed silica stabilizes the lithium/electrolyte interface, as shown by a lower polarization and interfacial resistance of a Li/composite-electrolyte/Li cell compared to a Li/baseline-electrolyte/Li cell. Also, Li(Ni)/electrolyte/Li cycling shows that a higher cycling efficiency is achieved with composite electrolytes; a full cell with composite electrolytes shows a higher discharge capacity and less capacity fading than that with a baseline electrolyte.

Although the fumed silica-surface chemistry does not affect the stabilizing effect on the lithium-solvent interface, it does affect the extent of stabilization. The most improved interfacial stability from Li/electrolyte/Li and full cell cycling results is seen between lithium and A200 with hydroxyl surface groups. The improvement effect increases with the increasing content of fumed silica.

## Acknowledgments

We gratefully acknowledge funding from the Department of Energy, Office of Basic Energy Sciences and Office of Transportation Technologies. We also thank 3M for providing LiTFSI salt, Degussa for supplying fumed silica, OM Group, Inc., for giving us $LiCoO_2$, and the Baker group at Michigan State University for synthesizing EO-modified fumed silica.

*North Carolina State University assisted in meeting the publication costs of this article.*

## References

1. G. B. Appetecchi, S. Scaccia, and S. Passerini, *J. Electrochem. Soc.*, **147**, 4448 (2000).
2. G. B. Appetecchi, F. Croce, L. Persi, F. Ronci, and B. Scrosati, *Electrochim. Acta*, **45**, 1481 (2000).
3. F. Capuano, F. Croce, and B. Scrosati, *J. Electrochem. Soc.*, **138**, 1918 (1991).
4. B. Kumar and L. G. Scanlon, *J. Power Sources*, **52**, 261 (1994).
5. J. Fan and P. S. Fedkiw, *J. Electrochem. Soc.*, **144**, 399 (1997).
6. J. Fan, S. R. Raghavan, X. Y. Yu, S. A. Khan, P. S. Fedkiw, J. Hou, and G. L. Baker, *Solid State Ionics*, **111**, 117 (1998).
7. M. C. Borghini, M. Mastragostino, S. Passerini, and B. Scrosati, *J. Electrochem. Soc.*, **142**, 2118 (1995).
8. J. E. Weston and B. C. H. Steele, *Solid State Ionics*, **7**, 75 (1982).
9. S. Skaarup, K. West, and B. Zachauchristiansen, *Solid State Ionics*, **28**, 975 (1988).
10. J. Plocharski and W. Wieczorek, *Solid State Ionics*, **28**, 979 (1988).
11. J. Plocharski, W. Wieczorek, J. Przyluski, and K. Such, *Appl. Phys. A: Mater. Sci. Process.*, **49**, 55 (1989).
12. B. K. Choi, Y. W. Kim, and K. H. Shin, *J. Power Sources*, **68**, 357 (1997).
13. Y. Dai, Y. Wang, S. G. Greenbaum, S. A. Bajue, D. Golodnitsky, G. Ardel, E. Strauss, and E. Peled, *Electrochim. Acta*, **43**, 1557 (1998).
14. F. Croce, R. Curini, A. Martinelli, L. Persi, F. Ronci, B. Scrosati, and R. Caminiti, *J. Phys. Chem. B*, **103**, 10632 (1999).
15. W. Wieczorek, K. Such, H. Wycislik, and J. Plocharski, *Solid State Ionics*, **36**, 255 (1989).
16. B. Scrosati, F. Croce, and L. Persi, *J. Electrochem. Soc.*, **147**, 1718 (2000).
17. B. Kumar, S. J. Rodrigues, and L. G. Scanlon, *J. Electrochem. Soc.*, **148**, A1191 (2001).
18. S. A. Khan, G. L. Baker, and S. Colson, *Chem. Mater.*, **6**, 2359 (1994).
19. H. J. Walls, J. Zhou, J. A. Yerian, P. S. Fedkiw, S. A. Khan, M. K. Stowe, and G. L. Baker, *J. Power Sources*, **89**, 156 (2000).
20. S. R. Raghavan, M. W. Riley, P. S. Fedkiw, and S. A. Khan, *Chem. Mater.*, **10**, 244 (1998).
21. G. Michael and H. Ferch, *Basic Characteristics of Aerosil*, Degussa Technical Bulletin Pigment No. 11, Degussa, Akron, OH (1998).
22. H. Barthel, L. Rosch, and J. Weis, in *Organosilicon Chemistry II. From Molecules to Materials*, N. Auner and J. Weis, Editors, p. 761, VCH, Weinheim (1996).
23. J. Hou, Ph.D. Thesis, University of Michigan, Ann Arbor, MI (1997).
24. R. K. Iler, *The Chemistry of Silica: Solubility, Polymerization, Colloid and Surface Properties, and Biochemistry*, p. 172, John Wiley & Sons, New York (1979).
25. H. J. Walls, P. S. Fedkiw, S. A. Khan, and T. A. Zawodzinski, Jr., *J. Electrochem. Soc.*, To be submitted.
26. J. Fan and P. S. Fedkiw, *J. Power Sources*, **72**, 165 (1998).
27. D. Aurbach, Y. Gofer, and J. Langzam, *J. Electrochem. Soc.*, **136**, 3198 (1989).
28. D. Fauteux, *Solid State Ionics*, **17**, 133 (1985).
29. F. Croce, L. Persi, F. Ronci, and B. Scrosati, *Solid State Ionics*, **135**, 47 (2000).
30. G. B. Appetecchi, F. Croce, G. Dautzenberg, M. Mastragostino, F. Ronci, B. Scrosati, F. Soavi, A. Zanelli, F. Alessandrini, and P. P. Prosini, *J. Electrochem. Soc.*, **145**, 4126 (1998).
31. S. R. Raghavan, J. Hou, G. L. Baker, and S. A. Khan, *Langmuir*, **16**, 1066 (2000).
32. H. Ferch, *The Use of Hydrophobic Aerosil in the Coatings Industry*, Degussa Technical Bulletin Pigments No. 18, Degussa, Akron, OH (1993).
33. S. R. Raghavan, H. J. Walls, and S. A. Khan, *Langmuir*, **16**, 7920 (2000).
34. J. Przyluski, M. Siekierski, and W. Wieczorek, *Electrochim. Acta*, **40**, 2101 (1995).
35. W. Wieczorek, Z. Florjanczyk, and J. R. Stevens, *Electrochim. Acta*, **40**, 2251 (1995).
36. M. Arakawa, S. Tobishima, Y. Nemoto, M. Ichimura, and J. Yamaki, *J. Power Sources*, **43**, 27 (1993).
37. W. K. Behl and E. J. Plichta, *J. Power Sources*, **72**, 132 (1998).
38. L. J. Krause, W. Lamanna, J. Summerfield, M. Engle, G. Korba, R. Loch, and R. Atanasoski, *J. Power Sources*, **68**, 320 (1997).
39. X. Wang, E. Yasukawa, and S. Mori, *Electrochim. Acta*, **45**, 2677 (2000).